

# Light Transfer in a Bubble Sparged Photobioreactor for Simultaneous Hydrogen Production and $CO_2$ Mitigation

by Halil Berberoglu, Juan Yin, and Laurent Pilon\*

Mechanical and Aerospace Engineering Department  
Henri Samueli School of Engineering and Applied Science  
University of California, Los Angeles - Los Angeles, CA 90095, USA  
\* Corresponding Author Phone: +1 (310) 206-5598, E-mail: pilon@seas.ucla.edu

## Abstract

This paper presents a parametric study of light transfer simulations in a rectangular photobioreactor containing gas bubbles and cyanobacteria *Anabaena variabilis* suspended in water. To the best of our knowledge, this paper presents for the first time a model for such system (i) using a consistent set of radiative properties of the medium derived from experimental data and from Mie theory, (ii) accounting for anisotropic scattering by two types of scatterers namely the bubbles and filamentous microorganisms, and (iii) considering the spectral dependency of radiation characteristics in the spectral range from 400 to 700 nm using a box model. The steady-state one-dimensional radiation transfer equation is solved using the modified method of characteristics. Parameters studied include the bacteria concentration, the bubble radius and void fraction, as well as the scattering phase function. It was established that the strongly forward scattering by the bubbles must be accounted for and the truncated phase function is recommended. In the absence of bubbles ignoring forward scattering by the bacteria leads to errors as high as 20%.

## 1. INTRODUCTION

Increased amounts of greenhouse gas emissions as well as the exhaustion of cheap fossil fuel resources are calling for clean and renewable energy sources. Hydrogen, to be used in fuel cells, is considered to be an attractive alternative fuel since water vapor is the only byproduct from its reaction with oxygen. Photo-biological hydrogen production by cultivation of cyanobacteria (or green algae) offers a clean and sustainable alternative to thermochemical or electrolytic production technologies. The cyanobacterium *A. variabilis* is a filamentous cyanobacteria which uses carbon dioxide as its carbon source and sunlight as its energy source. It harvests the light energy in the spectral range from 400 to 700 nm, known as the photosynthetically active radiation or PAR. In turn, *A. variabilis* produces oxygen, hydrogen and grows to form filaments of approximately 5  $\mu m$  in diameter and 100  $\mu m$  in length (Fig. 1(a)).

Limited light penetration, dissolved oxygen accumulation, and limited carbon dioxide availability to the microorganisms are the major factors affecting the performance of a photobioreactor for the production of hydrogen [1]. Mass transfer limitations can be overcome by sparging

the photobioreactor with carbon dioxide bubbles. However, sparging affects the light transfer within the photobioreactor due to light scattering by the bubbles. Therefore, it is necessary to model and analyze the effects of the presence of both bubbles and microorganisms on light transfer in order to optimize the design and operation of hydrogen producing photobioreactors.

Pioneering work in simulating light transfer in micro-algal ponds was published by Daniel *et al.* [2]. They used the radiative transport equation (RTE) at a single wavelength and accounted only for the presence of unicellular algae. The authors estimated the scattering phase function of unicellular algae with a weighted sum of thirty Legendre polynomials to be used in the RTE. They recommended using the six-flux approximation for solving the RTE. Moreover, the authors concluded that scattering is unimportant when the single scattering albedo is less than 0.5 and scattering is strongly in the forward direction. In addition, Kim *et al.* [3] modelled light transfer in a sulfate reducing photobioreactor using Beer-Lambert's law. The authors defined an effective extinction coefficient accounting for light absorption by bacteria and light scattering by the sulphur crystals excreted by bacteria. In addition, Cornet *et al.* [4] applied the RTE to model the light transfer for cultivating filamentous cyanobacterium *Spirulina platensis* accounting for absorption and isotropic scattering by the microorganisms. The absorption and scattering coefficients of the microorganisms were obtained from experimental data. The RTE was solved using the Schuster-Schwarzschild two-flux approximation. Finally, their model did not account for the spectral dependency of the radiation characteristics and for the strongly forward scattering.

The objective of this study is to maximize hydrogen production and carbon dioxide consumption by the microorganism *Anabaena variabilis* in a bubble sparged photobioreactor. The analysis presented here aims at modeling and simulating light transfer within the photobioreactor for various filamentous microorganism concentrations, bubble radius, and void fractions accounting for absorption and anisotropic scattering over the spectral range from 400 to 700 nm.

## 2. ANALYSIS

Let us consider a plane-parallel photobioreactor as shown schematically in Figure 1(b). The reactor contains the cyanobacterium *A. variabilis* at concentration  $X$  (concentration of bacteria with respect to the total volume of the reactor), expressed in kg dry cell/m<sup>3</sup>, and bubbles containing carbon dioxide with radii  $a$  and void fraction  $f_B$  offering large gas/liquid interfacial area for mass transfer. The microorganism concentration  $X$  ranges from 0.035 to 0.35 kg/m<sup>3</sup> as reported by Merzlyak and Naqvi [5]. The bubble radius  $a$  ranges from 25 to 500  $\mu\text{m}$  offering higher interfacial area than millimeter size bubbles for the same void fraction, thus increasing the mass transfer rate. Finally, the void fraction is such that  $0 \leq f_B \leq 0.3$  so bubbly flow prevails. The reactor is considered to be illuminated only from the top with diffuse intensity  $I_o$ . As the light penetrates into the photobioreactor, it is absorbed by the liquid phase and the microorganisms and scattered anisotropically by both the bubbles and the microorganisms.

### 2.1. Assumptions

In order to make the problem mathematically trackable it is assumed that: (1) light transfer is one-dimensional, (2) steady-state radiation transfer prevails, (3) the microorganisms, and the bubbles are uniformly distributed in the reactor, (4) the bubbles and microorganisms are monodisperse, (5) the liquid phase is cold, weakly absorbing, and non-scattering, (6) the optical properties of the liquid phase are those of pure water, (7) the gas bubbles are non absorbing

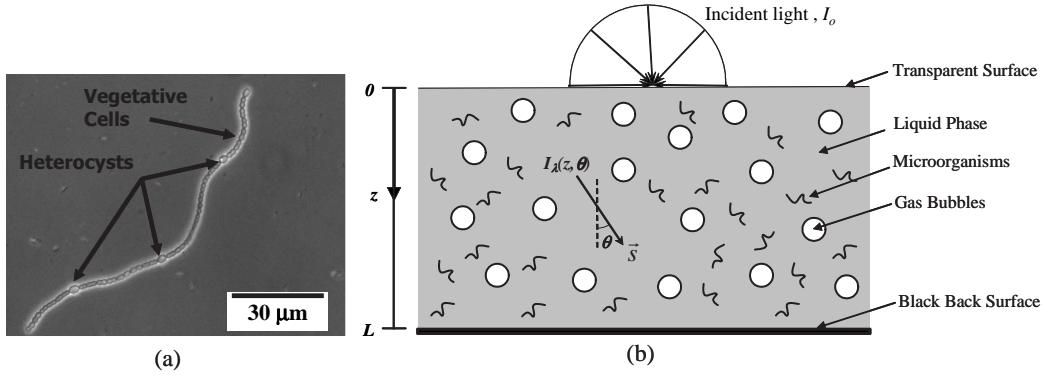


Fig. 1 (a) Micrograph of *A. variabilis* (b) schematic of the photobioreactor system considered.

but only scattering particles, (8) the phase function of bubbles is computed from the Mie theory assuming the liquid phase is non-absorbing and bubbles are spherical, (9) the scattering phase function of the filamentous microorganisms is that of a medium consisting of randomly oriented infinitely long fibers embedded in water, (10) independent scattering prevails for both the microorganisms and the bubbles. Studies by Tien and Drolen [6] and Lee [7] confirm this assumption for the ranges of parameters under consideration, and (11) the photobioreactor's top surface is treated as non-reflecting.

## 2.2. Governing Equation

The radiative transfer equation (RTE) is an energy balance on the radiative energy traveling in a particular direction  $\vec{s}$ . Considering the in-scattering by microorganisms and bubbles separately, the steady-state RTE can be written as,

$$\frac{\partial I_\lambda(z, \vec{s})}{\partial z} = -\kappa_{eff,\lambda} I_\lambda(z, \vec{s}) - \sigma_{eff,\lambda} I_\lambda(z, \vec{s}) + \frac{\sigma_{X,\lambda}}{4\pi} \int_{4\pi} I_\lambda(z, \vec{s}_i) \Phi_{X,\lambda}(\vec{s}_i, \vec{s}) d\Omega_i + \frac{\sigma_{B,\lambda}}{4\pi} \int_{4\pi} I_\lambda(z, \vec{s}_i) \Phi_{B,\lambda}(\vec{s}_i, \vec{s}) d\Omega_i \quad (1)$$

where  $I_\lambda(z, \vec{s})$  is the radiation intensity in the direction  $\vec{s}$  at location  $z$ , and  $\kappa_{eff,\lambda}$  and  $\sigma_{eff,\lambda}$  are the effective spectral absorption and scattering coefficients, respectively. The coefficients  $\sigma_{X,\lambda}$  and  $\sigma_{B,\lambda}$  are the spectral scattering coefficients of the microorganisms and the bubbles, respectively. The scattering phase functions of bacteria,  $\Phi_{X,\lambda}$ , and bubbles,  $\Phi_{B,\lambda}$ , describe the probability that radiation travelling in the solid angle  $d\Omega_i$  around the direction  $\vec{s}_i$  will be scattered into the solid angle  $d\Omega$  around direction  $\vec{s}$ . The effective absorption coefficient  $\kappa_{eff,\lambda}$  accounts for the absorption by the liquid phase and by the microorganisms at wavelength  $\lambda$ . It can be written in terms of the void fraction  $f_B$  and of the microorganism concentration  $X$  as  $\kappa_{eff,\lambda} = \kappa_{L,\lambda}(1 - f_B - Xv_X) + A_{abs,\lambda}X$ , where  $v_X$  is the specific volume of cyanobacteria equal to  $0.001 \text{ m}^3/\text{kg}$ . The absorption coefficient of the liquid phase  $\kappa_{L,\lambda}$  is expressed in  $\text{m}^{-1}$ , and the mass absorption cross-section of microorganisms  $A_{abs,\lambda}$  is expressed in  $\text{m}^2/\text{kg}$ . The term  $A_{abs,\lambda}X$  corresponds to the absorption coefficient of microorganisms  $\kappa_{X,\lambda}$ . Finally, The term  $Xv_X$  represents the volume fraction of photobioreactor occupied by microorganisms and has a maximum value of  $3.5 \times 10^{-4}$ .

Assuming independent scattering, the effective scattering coefficient of the composite medium  $\sigma_{eff,\lambda}$  can be expressed as the sum of the scattering coefficients of the microorganisms  $\sigma_{X,\lambda}$  and

of the bubbles  $\sigma_{B,\lambda}$ ,  $\sigma_{eff,\lambda} = \sigma_{X,\lambda} + \sigma_{B,\lambda} = S_{sca,\lambda}X + (3f_B/4a)Q_{sca,B}(a, \lambda)$ , where  $S_{sca,\lambda}$  is the mass scattering cross-section of microorganisms expressed in  $m^2/kg$  and  $Q_{sca,B}(a, \lambda)$  is the scattering efficiency factor of monodispersed bubbles of radius  $a$  at wavelength  $\lambda$  obtained from the Mie theory. Note that  $3f_B/a$  is the interfacial area concentration  $A_i$  of the bubbles and  $\sigma_{B,\lambda}$  can alternatively be written as  $\sigma_{B,\lambda} = (A_i/4)Q_{sca,B}(a, \lambda)$ .

Finally, the reactor is illuminated with a diffuse light source only from the top and the back surface is assumed to be cold and black. Therefore, the boundary conditions for Equation (1) can be written as  $I_\lambda(0, \theta) = I_{o,\lambda}$  for  $0 \leq \theta < \pi/2$  and  $I_\lambda(L, \theta) = 0$  for  $\pi/2 < \theta < \pi$ , where  $I_\lambda$  is the intensity of sunlight at  $\lambda$ . The Sun is assumed to be a blackbody at temperature 5800 K and the total irradiance incident on the photobioreactor is assumed to be  $146.71 \text{ W/m}^2$  in the PAR [8].

### 2.3. Closure Laws

#### The Microorganisms

In order to simplify the numerical simulations, the values of the spectral quantities needed to solve Equation (1) are estimated using the box model [8]. This model approximates a spectral quantity with a series of boxes of width  $\Delta\lambda$  and height  $\kappa_{X,\lambda_c}$  centered around the wavelength  $\lambda_c$  such that the area under the original spectrum equals the area under the box [8]. Fig. 2 shows the reported spectral absorption and scattering coefficients of *A. variabilis* [5].

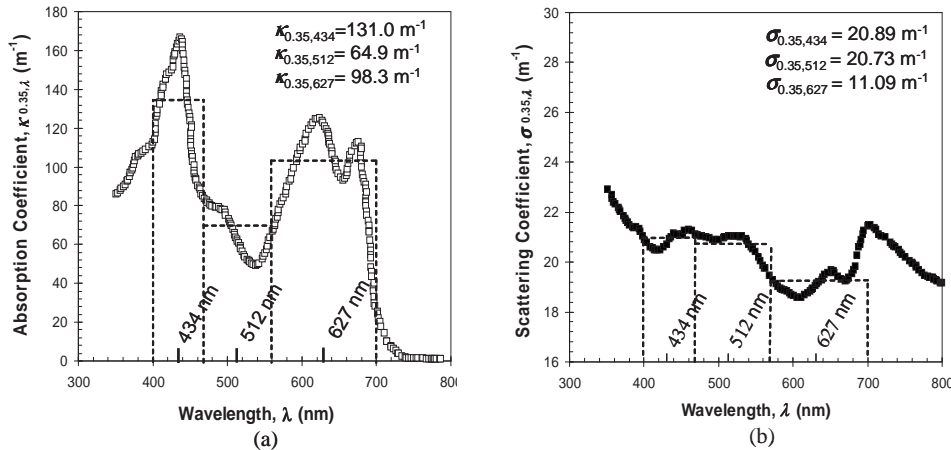


Fig. 2 The box model applied to the (a) absorption and (b) scattering coefficients of *A. variabilis* at concentration  $0.35 \text{ kg/m}^3$  in the photosynthetically active part of the spectrum [5].

The absorption spectrum of *A. variabilis* is approximated using three boxes with wavelength intervals from 400 to 469 nm, 469 to 556 nm and 556 to 700 nm. The center wavelengths of the boxes are assigned at the midpoint of each box at 434, 512, and 627 nm. Boxes 1 and 3 capture the absorption peaks corresponding to electron production for photosynthesis and hydrogen production.

The box absorption and scattering coefficients of *A. variabilis* are calculated using the data reported by Merzlyak and Naqvi [5] and our calibration experiments performed for various microorganism concentrations and presented in Figures 3. They indicate that both absorption and scattering coefficients are proportional to the microorganism concentration  $X$ . The slopes of the linear fits to these curves represent the mass absorption  $A_{abs,\lambda_c}$  and mass scattering  $S_{sca,\lambda_c}$  cross-sections of *A. variabilis* for a given box centered around  $\lambda_c$ . The scattering cross-section

of *A. variabilis* in boxes 1 and 2 do not differ appreciably as shown in Fig. 3(b).

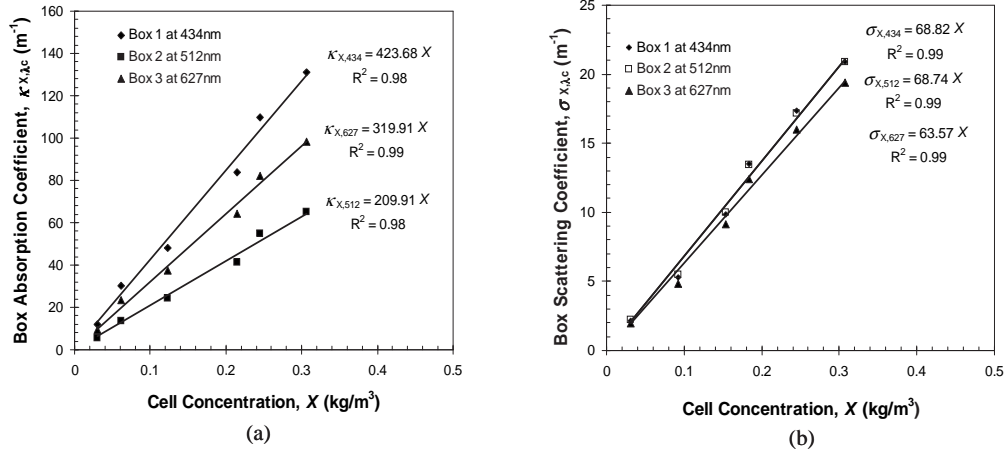


Fig. 3 Variations of (a) absorption and (b) scattering coefficients versus bacteria concentration [5].

The values of the radiation characteristics associated with the liquid phase, the microorganisms, and the bubbles approximated with the box model are summarized in Table 1.

Tab. 1 Summary of optical properties and boundary conditions for each box.

Box	Center Wavelength $\lambda_c$ (nm)	Liquid Phase		Bubbles $Q_{sca,B}$	Microorganisms				B.C. $I_{0,\lambda_c}$ ( $W m^{-2} sr^{-1}$ )
		$n_{L,\lambda_c}$	$\kappa_{L,\lambda_c}$ ( $\times 10^3 m^{-1}$ )		$n_{X,\lambda_c}$	$k_{X,\lambda_c}$ $\times 10^3$	$A_{abs,\lambda_c}$ ( $m^2/kg$ )	$S_{sca,\lambda_c}$ ( $m^2/kg$ )	
1	434	1.33	35.9	1.0	1.41	10.09	423.68	68.82	5.44
2	512	1.33	30.9	1.0	1.41	6.37	319.91	68.74	7.22
3	627	1.33	283.4	1.0	1.41	2.73	209.91	63.57	10.69

Finally, the scattering phase function of *A. variabilis* is assumed to be that of randomly oriented infinite fibers embedded in water [Assumption (9)]. The code implementing the Mie theory for normally incident radiation on a single infinitely long cylinder is given by Bohren and Huffman [9]. This code is modified to calculate the scattering phase function of a medium of randomly oriented infinitely long cylinders and has been successfully validated against the results reported by Lee [10]. The absorption index of water is on the order of  $10^{-9}$  and taken as zero and the refractive index is taken as 1.33. The values of the refractive index in each box  $n_{X,\lambda_c}$  and of the absorptive index  $k_{X,\lambda_c}$  of bacteria, are obtained from Stramski and Mobley [11]. Their values are reported in Table 1. The results of the Mie theory indicate that the scattering phase function does not change appreciably over the spectral range of interest and for the size parameter of microorganisms such that  $22 \leq \chi_X \leq 39$ .

Alternatively, the phase function can be approximated as a Henyey-Greenstein phase function (HG). The asymmetry factor  $g_X = 0.9919$  was computed using the results of the Mie theory according to  $g_X = \frac{1}{4\pi} \int_{4\pi} \Phi_X(\Theta) \cos(\Theta) d\Omega$ . The phase function can also be expressed as a truncated phase function (TPF) as suggested by Baillis *et al.* [12]. In this model  $\Phi(\Theta)$  is divided in two parts, from 0 to  $\Theta_{cutoff}$  and from  $\Theta_{cutoff}$  to  $\pi$ . Each part is a linear combination of two HG phase functions with parameters  $g_{TPF,1}$ , and  $g_{TPF,2}$ . The TPF is expressed as,

$$\begin{aligned} \Phi(\Theta) &= f_1 \Phi_{HG,g_{TPF,1}}(\Theta) + (1 - f_1) \Phi_{HG,g_{TPF,2}} & \text{for } 0 \leq \Theta \leq \Theta_{cutoff} \\ \Phi(\Theta) &= h_1 [f_1 \Phi_{HG,g_{TPF,1}}(\Theta) + (1 - f_1) \Phi_{HG,g_{TPF,2}}] & \text{for } \Theta_{cutoff} < \Theta < \pi \end{aligned} \quad (2)$$

where  $f_1$  is a weight parameter and  $h_1$  is a fitting parameter. The parameters  $f_1$ ,  $h_1$ ,  $\Theta_{\text{cutoff}}$ ,  $g_{TPF,1}$ , and  $g_{TPF,2}$  are determined by minimizing the sum of the squares of the error between the Mie theory calculations and the TPF model. The parameters are found to be  $f_1 = 0.104$ ,  $h_1 = 0.4$ ,  $\Theta_{\text{cutoff}} = \pi/3$ ,  $g_{TPF,1} = 0.99997$ , and  $g_{TPF,2} = 0.992$ . Equation (2) is normalized by the method previously adopted by Nicolau *et al.*[13]. Fig. 4(a) shows the phase functions of *A. variabilis* calculated by (i) Mie theory, (ii) the HG phase function and (iii) the TPF corresponding to  $\lambda_c = 512$  nm and size parameter  $\chi_X = 30$ .

### The Bubbles

The scattering efficiency factor  $Q_{sca,B}(a, \lambda)$  and the scattering phase function  $\Phi_B(\Theta)$  of the bubbles are predicted by the Mie theory calculations using the code provided by Bohren and Huffman [9] for a sphere of radius  $a$  and refractive index 1 embedded in water with  $n_L = 1.33$ . The results indicate that  $Q_{sca,B}(a, \lambda)$  is equal to 1.0 (corrected for the diffraction paradox) and does not vary more than 0.4% for the bubble size parameters  $224 \leq \chi_B \leq 2356$  in the PAR. Therefore, the scattering coefficient for the bubbles is independent of the wavelength and can be written as,  $\sigma_{B,\lambda} = 0.75f_B/a$ . Similarly, it was found that  $\Phi_B(\Theta)$  does not vary appreciably for the size parameters considered. Moreover, in order to simplify the calculations, the phase function obtained from Mie theory is approximated by the HG phase function with asymmetry factor equal to  $g_B = 0.8768$ . Alternatively,  $\Phi_B(\Theta)$  can be estimated by the TPF with parameters  $f_1 = 0.6$ ,  $h_1 = 0.1$ ,  $\Theta_{\text{cutoff}} = \pi/2$ ,  $g_{TPF,1} = 0.996$ , and  $g_{TPF,2} = 0.55$ . Fig. 4(b) compares the phase functions obtained by (i) the Mie theory, (ii) the HG phase function, and (iii) the TPF for a bubble of size parameter  $\chi_B = 1500$  at wavelength  $\lambda = 512$  nm.

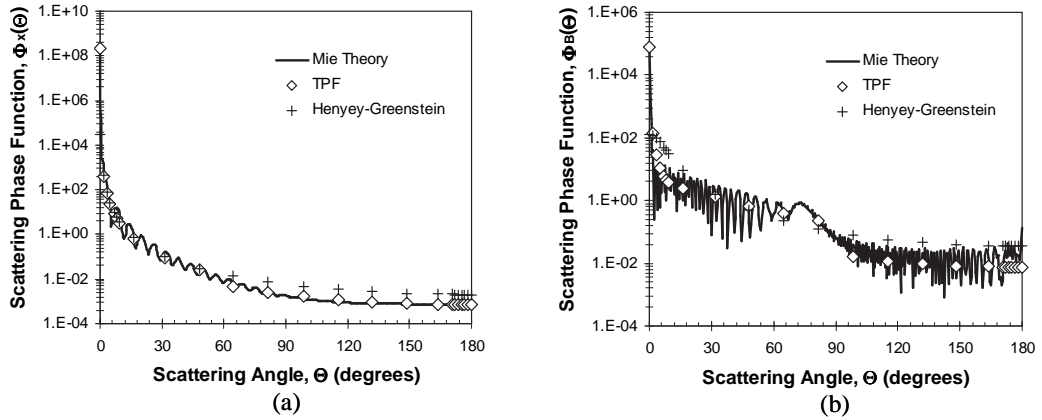


Fig. 4 Comparison of the exact and approximate phase functions for (a) *A. variabilis* and (b) a bubble of size parameter  $\chi_B = 1500$  submerged in water.

### The Liquid Phase

The optical properties of the liquid phase are assumed to be those of pure water [Assumption (6)]. The values of refractive and absorption index of water are obtained from Ref. [14] and approximated with the box model. The refractive index of water,  $n_L$ , is fairly constant and equal to 1.33 throughout the PAR. The absorption coefficient of the liquid phase  $\kappa_{L,\lambda}$  is proportional to the absorption index of water  $k_{L,\lambda}$  and defined as  $\kappa_{L,\lambda} = 4\pi k_{L,\lambda}/\lambda$ . As presented in Table 1, the maximum value of  $\kappa_{L,\lambda}$  is  $0.283 \text{ m}^{-1}$  which is an order of magnitude smaller than the absorption coefficient of microorganisms at their lowest concentration  $X = 0.035 \text{ kg/m}^3$ . Therefore, the contribution of  $\kappa_{L,\lambda}$  to  $\kappa_{eff,\lambda}$  can be ignored and  $\kappa_{eff,\lambda}$  becomes only a function of the microorganism concentration.

## 2.4. Method of Solution

The modified method of characteristics [15] is employed to solve Equation (1). It consists of transforming a hyperbolic partial differential equation into a set of ordinary differential equations which are solved along the characteristic curves of the photons. It makes use of an arbitrary set of points and traces particles backward in space from each point. These equations are solved using the fourth order Runge-Kutta method at every point and in 24 discrete directions of the Gaussian quadrature used by Baillis *et al.* [12]. The integrals for the in-scattering terms and the local flux (or fluence)  $G_{\lambda_c}(z)$  are computed as sums using the weights of the quadrature [12]. Finally, the spectral flux is calculated for each of the three boxes and summed up to give the total flux in the PAR defined as  $G_{PAR}(z) = G_{434}(z) + G_{512}(z) + G_{627}(z)$ . The total flux  $G_{PAR}(z)$  can then be used to model the growth rate of bacteria population.

## 3. RESULTS AND DISCUSSION

Simulations have been performed for low ( $X = 0.035 \text{ kg/m}^3$ ) and high ( $X = 0.35 \text{ kg/m}^3$ ) microorganism concentrations at three different interfacial area concentrations  $A_i$  namely 0, 450, and  $1,500 \text{ m}^{-1}$ . Each parameter combination has been simulated for four different approaches (i) neglecting the in-scattering term, (ii) assuming isotropic scattering for bubbles and microorganisms, and (iii) accounting for anisotropic scattering by both scatterers using the HG phase function, and (iv) the TPF. To assess the overall contribution of the scattering, the average single scattering albedo  $\omega_{\text{eff}} = \int_{PAR} \sigma_{\text{eff}} d\lambda / \int_{PAR} (\sigma_{\text{eff}} + \kappa_{\text{eff}}) d\lambda$  is calculated.

The results for the total flux  $G_{PAR}(z)$  normalized by the total incident flux,  $G_{PAR,in} = 146.71 \text{ W/m}^2$ , are presented in Fig. 5. For the sake of clarity results within the first 20 mm are presented for high bacteria concentration simulations. Since the objective of the study is to determine the availability of light to microorganisms in the photobioreactor and to facilitate effective comparison of the results, the concept of penetration depth is also introduced. It is arbitrarily defined as the distance from the illuminated surface at which the flux decreases below 20% of the total irradiance of  $146.71 \text{ W/m}^2$  in the PAR. The results of simulations assuming isotropic scattering, ignoring in-scattering, and accounting for anisotropic scattering are summarized in Table 2.

Tab. 2 Summary of the simulation results.

Fig. 5	Parameters			Penetration Depth (mm)				$[G_{PAR}(0) - G_{PAR,in}]/G_{PAR,in}$		
	$A_i$	$X$	$\omega_{\text{eff}}$	TPF	HG	Iso.	No In-sca.	TPF	HG	Iso.
(a)	low	low	0.18	77.5	77.5	73.1	62.8	0%	0%	5%
(b)	low	high	0.18	7.8	7.8	7.4	6.3	0%	0%	5%
(c)	medium	low	0.91	76.8	62.9	32.4	6.3	1%	22%	55%
(d)	medium	high	0.55	7.6	7.6	6.2	3.3	0%	4%	20%
(e)	high	low	0.97	47.0	47.0	19.4	2.1	3%	39%	71%
(f)	high	high	0.78	7.2	7.2	2.4	1.6	0%	10%	37%

Figs. 5(a) and (b) compare the four models for scattering by the microorganisms in the absence of bubbles in the photobioreactor. They indicate that the computed penetration depth assuming isotropic scattering by microorganisms does not differ more than 6% from the case when anisotropic scattering is accounted for. However, ignoring in-scattering gives deviations as high as 20% for the penetration depth with respect to the anisotropic in-scattering case. On the other hand, the results for HG phase function and TPF does not differ appreciably. The scattering albedo for cases simulated in Figures 5(a) and (b) are identical and equal to 0.18 indicating that absorption dominates over scattering. Indeed, Table 1 shows that mass absorption

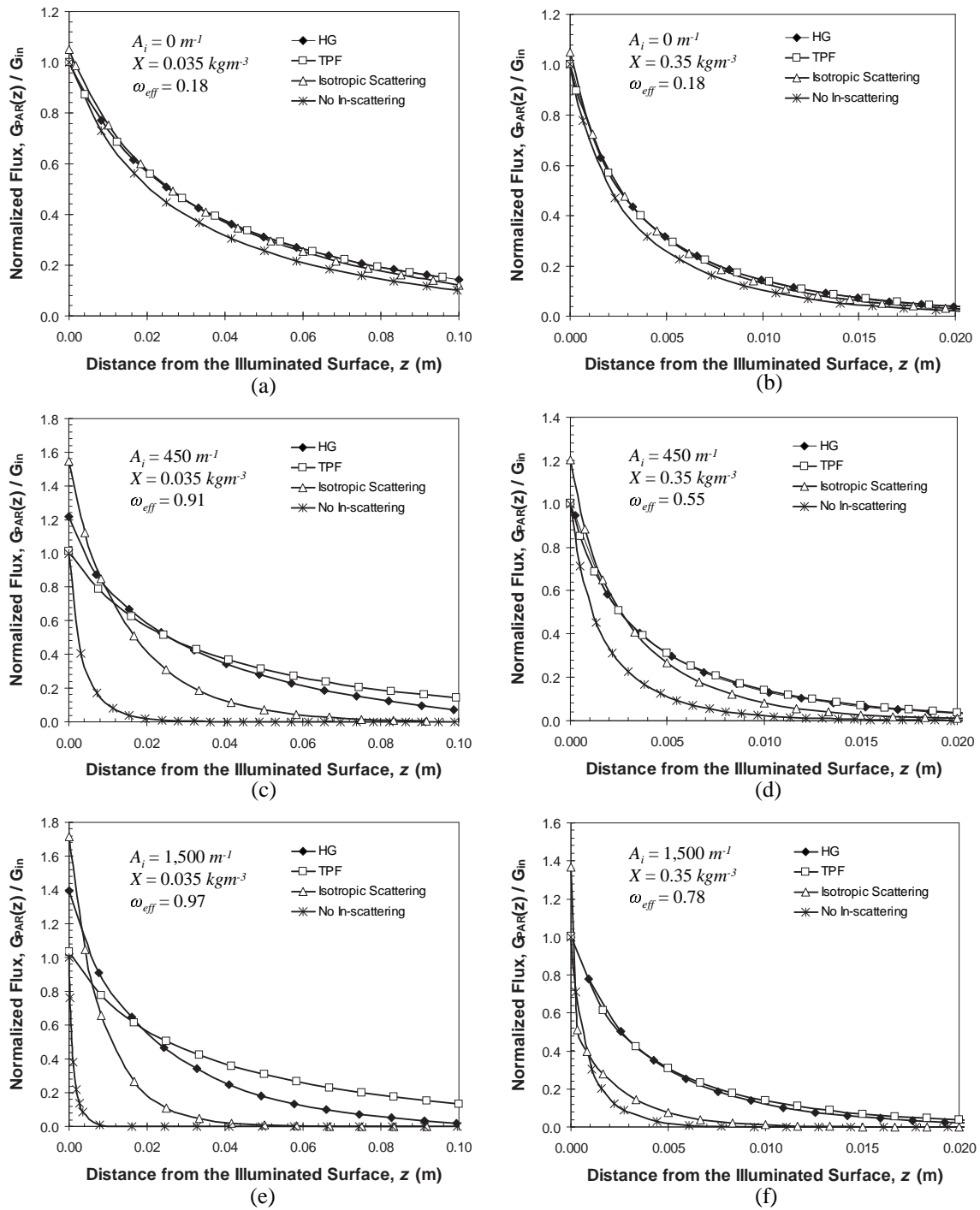


Fig. 5 Simulations results for interfacial area concentrations (i)  $0 \text{ m}^{-1}$  (ii)  $450 \text{ m}^{-1}$  and (iii)  $1,500 \text{ m}^{-1}$  and for low ( $X = 0.035 \text{ kg/m}^3$ ) and high ( $X = 0.350 \text{ kg/m}^3$ ) bacteria concentrations.

cross-section of *A. variabilis* is about an order of magnitude larger than that of scattering. However, for genetically engineered microorganisms with less pigments the absorption cross-section  $A_{abs,\lambda_c}$  decreases and anisotropic scattering effects are expected to be more significant.



Furthermore, Figs. 5(a), (c), and (e) as well as Table 2 show the effects of introducing bubbles into the photobioreactor. They establish that depending on the magnitude of the average scattering albedo,  $\omega_{\text{eff}}$ , different scattering phase function approximations can lead to significant deviations in the prediction of light transfer in the photobioreactor. For values of  $\omega_{\text{eff}}$  up to about 0.78, the predictions of the penetration depth using the HG and the TPF phase function approximations agree within 5.5% with each other. For  $\omega_{\text{eff}} = 0.91$  and 0.97 the deviations reach 18.1% and 37.4%, respectively. Moreover, either assuming isotropic scattering or neglecting in-scattering by the bubbles results in underestimation of the penetration depth by as much as 74.1% and 97.2%, respectively, compared with the TPF results. Therefore, for correctly modeling light transfer in bubble sparged photobioreactors, it is necessary to properly approximate the scattering phase function and account for the strongly forward scattering of the bubbles.

Finally, another effect of bubbles is to augment the total flux at the surface of the photobioreactor [ $G_{PAR}(z = 0)$ ] with respect to the total incident flux,  $G_{PAR,in} = 146.71 \text{ W/m}^2$ . The augmentation is greater for isotropic scattering than for forward scattering. For example, in the case of high interfacial area and low microorganism concentration [Fig. 5(e)] the flux at the top surface of the reactor is about 79% of  $G_{PAR,in}$  for the isotropic scattering assumption, 39% for the HG phase function, and 3% for the TPF. This can be attributed to the fact that bubbles scatter light strongly in the forward direction whereas isotropic scattering equally distributes light in all directions, that is backward as well as forward. On the other hand, the discrepancy between the HG and the TPF models is due to the over estimation of the back scattering by the HG as shown in Fig. 4(b).

#### 4. CONCLUDING REMARKS

This manuscript presented modeling of light transfer in a one-dimensional photobioreactor containing gas bubbles and filamentous cyanobacterium *Anabaena variabilis* suspended in water. Modeling was performed on a spectral basis using the box model and accounting for absorption by both *A. variabilis* and by the liquid phase as well as for anisotropic scattering by the bubbles and the bacteria. A consistent set of radiation characteristics for the bubbles and the microorganisms has been developed from experimental data and from Mie theory. The following conclusions can be drawn:

(1) Ignoring in-scattering or assuming isotropic scattering in a photobioreactor containing only *A. variabilis* underestimates light penetration by as much as 20% and 6%, respectively compared with cases accounting for anisotropic scattering.

(2) Increasing microorganism concentration decreases the discrepancies between the three scattering models. This is attributed to the fact that absorption dominates over scattering at high microorganism concentrations. Note that this might not be true for genetically engineered bacteria.

(3) It is necessary to account for anisotropic scattering for cases where the average scattering albedo  $\omega_{\text{eff}}$  is large. Therefore, assuming isotropic scattering or using Beer-Lambert law is not appropriate for predicting light transfer accurately in bubble sparged photobioreactors.

The model presented can be used in conjunction with mass transfer and microorganism growth models to design and optimize the reactor geometry and the sparging conditions for maximum hydrogen production and carbon dioxide consumption by bacteria.

## 5. ACKNOWLEDGEMENTS

The authors gratefully acknowledge the support of the California Energy Commission through the Energy Innovation Small Grant (EISG 53723A/03-29; Project Manager: Michelle McGraw).

### REFERENCES

- [1] J.R. BENEMANN, “Hydrogen production by microalgae”, *Journal of Applied Phycology*, vol. 12, pp. 291–300, 2000.
- [2] K.J. DANIEL, N.M. LAURENDEAU, and F.P. INCROPERA, “Prediction of radiation absorption and scattering in turbid water bodies”, *Journal of Heat Transfer*, vol. 101, pp. 63–67, 1979.
- [3] B.W. KIM, H.N. CHANG, I.K. KIM, and K.S. LEE, “Growth kinetics of the photosynthetic bacterium *chlorobium thiosulfatophilum* in a fed-batch reactor”, *Biotechnology and Bioengineering*, vol. 40, pp. 583–592, 1992.
- [4] J.F. CORNET, C.G. DUSSAP, J.B. GROSS, C. BINOIS, and C. LASSEUR, “A simplified monodimensional approach for modeling coupling between radiant light transfer and growth kinetics in photobioreactors”, *Chemical Engineering Science*, vol. 50, pp. 1489–1500, 1995.
- [5] M.N. MERZLYAK and K.R. NAQVI, “On recording the true absorption spectrum and scattering spectrum of a turbid sample: application to cell suspensions of cyanobacterium *Anabaena variabilis*”, *Journal of Photochemistry and Photobiology B: Biology*, vol. 58, pp. 123–129, 2000.
- [6] C. L. TIEN and B. L. DROLEN, “Thermal radiation in particulate media with dependent and independent scattering”, in *Annual Review of Numerical Fluid Mechanics and Heat Transfer*, T.C. Chawla, Ed., vol. 1, pp. 1–32. Hemisphere, New York, NY, 1987.
- [7] S.C. LEE, “Dependent vs independent scattering in fibrous composites containing parallel fibers”, *International Journal of Thermophysics and Heat Transfer*, vol. 8, pp. 641–646, 1994.
- [8] M. F. MODEST, *Radiative Heat Transfer*, Academic Press, San Diego, CA, 2003.
- [9] C.F. BOHREN and D.R. HUFFMAN, *Absorption and scattering of light by small particles*, John Wiley & Sons, New York, 1998.
- [10] S.C. LEE, “Scattering phase function for fibrous media”, *International Journal of Heat and Mass Transfer*, vol. 33, pp. 2183–2190, 1990.
- [11] D. STRAMSKI and C.D. MOBLEY, “Effect of microbial particles on oceanic optics: a database of single-particle optical properties”, *Limnology and Oceanography*, vol. 42, pp. 538–549, 1997.
- [12] H. RANDRIANALISOA, D. BAILLIS, and L. PILON, “Improved inverse method for radiative characteristics of closed-cell absorbing porous media”, *Journal of Thermophysics and Heat Transfer*, accepted 2005.
- [13] V.P. NICOLAU, M. RAYNAUD, and J.F. SACADURA, “Spectral radiative properties identification of fiber insulating materials”, *International Journal of Heat and Mass Transfer*, vol. 37, pp. 331–324, 1994.
- [14] G. M. HALE and M. R. QUERRY, “Optical constants of water in the 200-nm to 200- $\mu$ m wavelength region”, *Applied Optics*, vol. 12, pp. 555–563, 1973.
- [15] K. M. KATIKA and L. PILON, “Modified method of characteristics for transient radiative transfer”, *Journal of Quantitative Spectroscopy and Radiative Transfer*, vol. 98, pp. 220–237, 2006.